Manuscript prepared for Atmos. Chem. Phys.
with version 5.0 of the LaTeX class copernicus.cls.
Date: 17 May 2013

Rapid and sudden advection of warm and dry air in the Mediterranean basin

J. Mazon[1], **D. Pino**[1,2], **and M. Barriendos**[3]

[1]Applied Physics Department, BarcelonaTech (UPC), Barcelona, Spain
[2]Institute for Space Studies of Catalonia (IEEC–UPC), Barcelona, Spain.
[3]Institut Català de Ciències del Clima (IC3)

Correspondence to: J. Mazon (jordi.mazon@upc.edu)

Abstract. Rapid advection of extremely warm and dry air is studied during two events in the Mediterranean basin. On 27 August 2010 a rapid advection of extremely warm and dry air affected the northeast Iberian Peninsula during few hours. At the Barcelona city center, the temperature reached 39.3 °C, which is the maximum temperature value recorded during 230 years of daily data series. On 23 March 2008 a similar synoptic situation was the cause of a rapid increase of temperature and drop of relative humidity recorded for few hours in Heraklion (Crete). During the morning on that day the recorded temperature reaches 34 °C for several hours in the north coastline of this island.

According to the World Meteorological Organization none of these events can be classified as a heat wave, which requires at least two days of abnormally high temperatures; or as a heat burst as defined by the American Meteorological Society, where abnormal temperatures take place over a few minutes. For this reason, we suggest naming this type of event *flash heat*.

By using data from automatic weather stations in the Barcelona and Heraklion area and WRF mesoscale numerical simulations, these events are analyzed. Additionally, the primary risks and possible impacts on several fields are presented.

1 Introduction

The World20010 Meteorological Organization (WMO) defines a heat wave as a phenomenon in which the daily maximum temperature of more than five consecutive days exceeds the average maximum temperature by 5 °C with respect to the period 1961–1990 (Frich et al., 2012). The glossary of meteorology of the American Meteorological Society (AMETSOC, Glickman (2000)) defines a heat wave as a period of abnormally and uncomfortably hot and usually humid weather, which should last at least one day, but conventionally it lasts from several days to several weeks. The definition presents slight variations in the values of exceeded temperature with respect to the average temperature depending on the national weather service. However, a common characteristic is found in all regional definitions: speaking about a heat wave requires duration of at least 2 consecutive days of abnormal temperature values. Thus, heat waves are considered a synoptic phenomenon that cover several thousands of kilometers and last at least one day, but typically 2 or more days.

Many authors have studied the dynamics of heat waves and their effects in several fields, such as agriculture (Jolly et al., 2005), human health (Smoyer-Tomic et al., 2003; Meehl and Tebald, 2004), tourism (Steadman, 1984; Hamilton et al., 2005; Lise and Tol, 2002), energy consumption (Karl and Quayle, 1981; Hassid et al., 2000) and water demand (Smoyer-Tomic et al., 2003). Furthermore, several studies (Meehl and Tebald, 2004; Trenberth et al., 2007) show that an increase in intensity, frequency and the duration of heat waves around the Earth will occur during the XXI century. In all scenarios shown in the 4th IPCC report (Trenberth et al., 2007), the Mediterranean basin will be one of the most significant regions affected by an increase in both the intensity and frequency of heat waves during this century.

If a smaller scale is considered, the glossary of AMETSOC defines a heat burst as a rare atmospheric event characterized by gusty winds and a rapid increase in temperature and a decrease in relative humidity, typically occurring at night or in the early morning (Johnson, 1976; Glickman, 2000) and associated with descending air during a thunderstorm. A heat burst occurs only for a few minutes. Recorded temperatures during heat bursts have reached well above 32 °C,

sometimes rising by 11 °C or more within only a few minutes. Heat bursts are also characterized by extremely dry air and are sometimes associated with strong winds.

This paper aims to study two events associated with an increase in temperature and decrease in relative humidity occurring at intermediate temporal and spatial scales. Rapid advection of warm and dry air has been observed in several areas of the Mediterranean basin. We will call this phenomenon *flash heat*, because it occurs within a time scale shorter than a heat wave but longer than a heat burst. This event is usually associated with an adiabatic warming of downslope winds, associated to Foehn effect (Maninns and Sawford, 1979; Egger and Hoinka, 1992; Wakonigg, 1990).

However, the two studied cases here are associated to a rapid movement of a ridge from North Africa that shifted a warm and dry air mass from the Sahara desert. To our knowledge, there is no previous scientific reference naming this type of events. Table 1 summarizes the differences between the three types of abnormal high temperature events mentioned above. Note the different spatial and temporal scales of flash heat, as well as the dynamics of its formation.

The structure of this paper is as follows. Section 2 is devoted to analyze and describe by using observations and WRF mesoscale model numerical simulations the 27 August 2010 event in the northeast of the Iberian Peninsula, where a very warm and dry air mass affected this area over 8 hours. It focuses on the Barcelona area, where the maximum daily temperature in over 230 years was recorded. According to this analysis, a preliminary flash–heat definition is proposed in order to analyze the existence of similar flash–heat events during the XIX century in the daily temperature series of Barcelona (1790–2012). The rapid increase of temperature and decrease of relative humidity occurred on 23 March 2008 in Heraklion (Crete island) is analyzed in section 3. In section 4 we describe the main impacts that this event could produce on several fields, mainly in agriculture, energy demand, health and fires. Finally, in section 5 the main conclusions are presented.

2 The 27 August 2010 event (Barcelona event)

The summer of 2010 was the third warmest summer recorded in the Iberian Peninsula, according the Agency of Spanish Meteorology (AEMET). Particularly, August 2010 was the fifth warmest month since 1971; its mean temperature was 1.5 °C higher than the average monthly temperature and it was the third warmest month in this century. At the south and east of the Iberian Peninsula, maximum temperatures between 40 and 44 °C were recorded. Minimum early morning temperatures of between 23 and 26 °C were recorded by several official AEMET weather stations during this period.

However, the heat wave does not affect the north and northeast Iberian Peninsula. The warm and dry air mass was practically stationary, affecting the entire center and southern part of the Iberian Peninsula. But a rapid and brief movement of this warm air mass from the southeast to northeast on the 27 August 2010 affected the northeast Iberian Peninsula for several hours, when a significant increase in temperature was recorded as well as a decrease in the relative and absolute humidity. Automatic weather station located in the Barcelona city center recorded 39.3 °C (the highest temperature since 1780) and the relative humidity dropped to 19 %. In addition, the recorded temperature values from 1100 to 1600 UTC were above 30 °C, higher than 5 °C than the mean maximum temperature in August during the period 1961–1990, that has been 26.8 °C. However, for the 12 hours prior to and after than the hours in which the maximum value was recorded, the temperature remained within normal values. As will be shown, the period of abnormally high temperature could be considered as occurring from 1100 to 1600 UTC. This event cannot be classified according to the above definitions either as a heat wave or as a heat burst.

2.1 Synoptic situation

Fig.1 shows the temperature at 850 hPa obtained by the NCEP reanalysis at 0000 UTC from 26 to 28 August 2010. A ridge from North Africa remained stationary in Northwest Africa for a few days before the 25 August 2010, when it began to move to the north. On 25 August at 0000 UTC (not shown), the 25 °C isotherm at 850 hPa was located at the southern Iberian Peninsula and a large anticyclonic ridge was located in Northwest Africa. At the northern third of the Iberian Peninsula the 850–hPa isotherm was 15 °C at 0000 UTC. On 26 August, the ridge moved to the north. At 850 hPa (see Fig. 1a), the 25 °C–isotherm was in the central and southern Iberian Peninsula. On the 27, at 0000 UTC (Fig. 1b), the ridge (25 °C–isotherm at 850 hPa) extended from the southwest to the northeast of the Iberian Peninsula, and moved rapidly to the southeast, displaced by a northeast advection. On the 28 August, at 0000 UTC (see Fig. 1c), the border of the 25 °C–isotherm at 850 hPa was displaced to the southeast of the Iberian Peninsula. The 15 °C–isotherm at 850hPa approximately followed the Pyrenees Mountains. On the 29 of August the northeast advection increased, with a 10 °C–isotherm at 850 hPa at 0000 UTC over the Pyrenees (not shown). Several storms formed in the northeast Pyrenees during those days. In the south and southeast of the Iberian Peninsula, the heat wave continued, with temperatures between 20 °C and 25 °C at 850 hPa at the south and southeast until the 31 August 2010.

2.2 Analysis of surface observations

To avoid heat–island effect, data from the weather station installed at the Fabra Observatory, located 10 km away from the city center (420 masl) was selected. Fig. 2 shows the observed (closed symbols) temporal evolution during 27 August 2010 of temperature, relative humidity, wind

speed and direction. Fig. 2a shows that from approximately 0600 UTC to 1200 UTC the temperature increased by about 2.3 $^{\circ}\mathrm{C\,h^{-1}}$, from nearly 22 °C at 0500 UTC (a typical temperature value for this date and hour) to more than 36 °C at 1200 UTC. During this period the relative humidity dropped, from approximately 90 % at 0500 UTC to 20 % at 1200 UTC. From noon to 1600 UTC the relative humidity changed slightly. However, the temperature increased between 1200 and 1500 UTC, reaching the fifth historically high temperature recorded since 1914 in this observatory, 38.3 °C, at 1500 UTC. Until this hour wind direction (see Fig 2b) was approximately constant, around 270°. Therefore, westerly wind advected extreme warm and dry air mass from the inland of the Iberian Peninsula.

From approximately 1500 UTC, a change in wind direction occurred and western flow was replaced by easterly winds which removed the warm and dry air mass, advecting a relatively cold and wet Mediterranean air mass.This fact produced a decrease in temperature and a rise in relative humidity that can be clearly observed in Fig 2a. From 1500 UTC to 1600 UTC, the temperature dropped from 37 °C to 28 °C, and relative humidity rose from 20 % to nearly 60 %. From 1900 UTC on, normal values for this period of the year for both temperature and relative humidity were recorded. Consequently, the change in wind direction clearly drove the evolution of temperature and relative humidity.

2.3 Mesoscale numerical simulation

In order to analyze the dynamics of the atmosphere that produced this rapid change of temperature and relative humidity, the version 3.3 of the Advanced Research WRF–ARW (Skamarock et al., 2008) has been used. Four nested domains were defined with respective horizontal resolutions of 27, 9, 3 and 1 km. The smallest domain covers $70 \times 70\,\mathrm{km^2}$. The initial and boundary conditions were updated every six hours with data from the ECMWF operational analysis. The following parameterizations were used for the different physical processes: the Kain–Fritsch scheme in the two larger domains; no parameterization of cumulus formation in the two smallest domains; the MRF scheme for processes in the mixed layer; a simple ice scheme for the cloud microphysics; and cloud–radiation parameterization for the radiation parameterization. The simulation begins on the 25 August 2010 at 0000 UTC and finishes on the 28 at 1800 UTC.

In order to validate the simulation, Fig. 2 also shows the WRF simulated temperature, relative humidity, wind speed and direction (line and open symbols) at the nearest point of the model to the Fabra weather station. Both simulated temperature and relative humidity fit well the observed values. However, some discrepancies can be noticed in the maximum values. The maximum simulated temperature is around 35 °C, almost 3 °C less than the observed value. In addition, at 0500 and 0600 UTC the simulated temperature is around 3 °C higher than the observed one. Moreover, the simulated relative humidity overestimates the observed value at 1500 UTC. The simulated wind velocity and direction (not shown) also fit well the observations except the rapid change in wind direction recorded from 1500 UTC that occurs slowly in the WRF simulation.

According to the analysis of the simulation in domain 1 during the 25 and 26 August 2010 (not shown), a warm air mass was located in the southern part of the Iberian Peninsula. On the 27 August a west and southwest synoptic flow advected the warm air mass from the center and south of the Iberian Peninsula to the east and northeast region, where the maximum values of temperature were recorded on the 27 August.

Fig. 3 shows the simulated 2–m temperature (color contour) and the surface wind field (arrows) at the largest domain on the 27 August 2010. West and southwest synoptic flow advected warm and dry air mass from the center of the Iberian Peninsula to the northeast coast. The simulated maximum temperatures at 1000 UTC were located at the Mediterranean coast, with values of around 33–36 °C at the eastern and southeastern area, and 30–33 °C at the northeastern area, in agreement with the observed values by AEMET. During that day the intensity of the westerly flow prevented the formation of the sea breeze that usually helps to keep the temperature at moderate values in this area. At 1500 UTC (Fig. 3b) the westerly flow increased and the maximum recorded temperatures rose to 40 °C in many places of the coastline. According to the simulation, a northern advection affected the northern part of the Iberian Peninsula between 1700 and 1800 UTC. In this type of synoptic configuration, the flow turned northeast and east at the northeast coast of the Iberian Peninsula. At 1800 UTC (Fig. 3c) a relative cold and wet air mass from the northeast and east swept the warm and dry air mass, which cooled and moistened the air, decreasing the temperature to the usual values.

Figs. 4a–d shows the vertical cross section of temperature and water vapor–mixing ratio along the line AB defined in Fig. 4e at different hours. At 1000 UTC (Fig. 4a) a cold and dry air mass from the southwest arrives at the Mediterranean coastline, which remains stationary for approximately 4 hours (from 1000 to 1400 UTC). The relatively cold and wet Mediterranean air mass avoids the offshore displacement of the warm and dry air mass. Notice how in the boundary between both masses, the warm one rises vertically over the cold one. At 1200 UTC (Fig. 4b) a large gradient in temperature and humidity appears at the coastline of Barcelona. The simulated 2–m temperature reached more than 35 °C (see Fig. 4a) and the water vapor–mixing ratio lowered to $9\,\mathrm{g\,kg^{-1}}$. Around 10 km offshore from the coastline, the 2–m simulated temperature is around 26 °C and the water vapor–mixing ratio is around $16\,\mathrm{g\,kg^{-1}}$. The height of the accumulated warm air mass is estimated by looking at Fig. 4b, which is around 600 m. At 1500 UTC (Fig. 4c) the warm air moves offshore and displaces the relatively cold and wet Mediterranean air mass. This situation changed from 1800 UTC, as

is shown in Fig. 4d. The north advection shown in Fig. 3c ruled to the east at the Barcelona area, moistening and cooling the air while mixing the different layers and breaking the stratification. At 2000 UTC (not shown) the maritime flow restored the values of temperature and relative humidity.

2.4 Flash–heat definition and occurrence

According to the evolution of temperature observed during 27 August 2010 at the Barcelona area, a definition of flash heat event is suggested. An event of rapid increase of temperature could be considered as a flash heat if the following conditions are verified:

1. The maximum daily temperature (T_{max}) exceeds at least by 5 °C the absolute maximum temperature ($\overline{T}_{max-abs}$) averaged during the considered month in the period 1960–1990 ($T_{max} > 5+\overline{T}_{max-abs}$). This criterion follows the definition of heat wave by the WMO.

2. The temperature 24 hours prior to and later than the extreme temperature recorded (T_{24}) does not exceed the monthly average of the absolute maximum temperature ($T_{24} < \overline{T}_{max-abs}$). This criterion assures that the maximum temperature the day before and after the maximum daily temperature recorded remains in average values.

3. The temperature 12 hours prior to and after the extreme temperature recorded (T_{12}) does not exceed the 60th percentile of the monthly maximum average temperature ($T_{12} > p60\overline{T}_{max}$).

By using these criteria, table 2 shows the $\overline{T}_{max}$, $\overline{T}_{24}$, and $\overline{T}_{12}$ for a flash–heat event during July and August by using the recorded values at Fabra weather station during the period 1961–1990.

According to these data, a flash–heat event occurs during these summer months if:

1. The maximum daily temperature exceeds 37.6 °C in July and 36.6 °C in August.

2. The temperature 24 hours prior to and after the maximum daily–recorded temperature does not exceed 32.6 °C in July and 31.6 °C in August.

3. The temperature 12 hours prior to and after the maximum–recorded temperature does not exceed 28.6 °C in July and 27.6 °C in August

To know the frequency of these types of events, the definition of a flash–heat event has been applied to the daily temperature series of Barcelona starting from 1780. Although the series is not homogeneous (Mazon et al., 2011), a first approach to flash–heat events is possible by looking into a partial series of the daily temperature record. Table 3 shows some events detected as a flash heat during the XVIII and XIX centuries.

3 The 23 March 2008 event (Heraklion event)

The island of Crete, located at the middle–East part of the Mediterranean sea, near the north African coastline and consequently to the big Sahara desert, uses to be affected by advection of warm and dry air masses from the Sahara desert, also associated to intense dust events (Kaskaoutis et al., 2008; Fotiadi et al., 2006; Moulin et al., 1998). This advection produces an increase of temperature that only lasts several hours, especially at the north side of the island (Nastos, personal communication). Consequently, it cannot define this type of event as a heat wave.

3.1 Synoptic situation

On 21 March 2008 a low–pressure area was placed over the South of Greece around 1005 hPa at sea–level (not shown). A southwesterly flew to the Island of Crete. On 22 March this low pressure moved to South Turkey. At sea level, a southeast flow affected Crete. Figure 5 shows the temperature at 850 hPa obtained by the NCEP reanalysis on 22, 23 and 24 March 2008 at 0000 UTC. On 22 March (Fig. 5a) a warm air mass was located over North Africa. A ridge moved on 23 March to the north, affecting the whole island of Crete (Fig. 5b). On 24 March, the ridge moved out to the south (Fig. 5c).

3.2 Analysis of surface data

Data from the automatic weather station (39 masl, 35°19' N; 25°10' E) placed near Heraklion is used to detect this flash–heat event, and to validate the mesoscale numerical simulation. Fig. 6 shows the temporal evolution during 23 March 2008 of the observed temperature and relative humidity (closed symbols). During the early morning the observed temperature shows a large increase from 0300 UTC, reaching 30.2 °C at 0800 UTC. Relative humidity shows a large drop from 0400 UTC, reaching the minimum value around 20 % at 0800 UTC. From 1000 UTC temperature decreases and relative humidity increases gradually.

3.3 Mesoscale numerical simulation

WRF mesoscale model has been used to analyze the dynamics of the atmosphere that produced this rapid change of temperature and relative humidity. Three nested domains were defined with horizontal resolutions of 18, 6, and 2 km.The smallest domain covers 150×150 km^2. ECMWF operational analysis was used to provide the initial and boundary conditions every six hours. The same parameterizations physical parameterizations enumerated in section 2.3 were used for the mesoscale simulation of this event. The simulation begins on the 22 March 2008 at 0000 UTC and finishes on the 24 March at 1800 UTC.

The simulated evolution of 2–m temperature (blue line and open circles) and relative humidity (green dashed line and open triangles) at the nearest point of the model to the

Heraklion weather station is also shown in Fig. 6. A slight overestimation of temperature in the simulation is observed with respect the observations (around 2 °C) between 0700 to 1600 UTC. However, the simulated relative humidity shows a remarkable difference to the recorded values, especially from 1100 to 1900 UTC. While the recorded values of relative humidity between 1100 and 1700 UTC are around 70 %, the simulated values are lower than 50 %.

Fig 7 shows the simulated 2–m temperature (color contours) and surface wind field (arrows) at the smallest domain at several hours on 23 March 2008. At 0000 UTC (Fig. 7a) the simulation shows a southeasterly flow over the south coast of Crete, where the temperature was around 17 °C. However, at the north side a higher temperature, between 24 °C and 28 °C is simulated. At 0400 UTC (Fig. 7b) the southeasterly wind ruled to southerly; the warm and dry air mass associated to the North Africa advection, that can be considered as a warm front, lifted over the relatively cold sea air at around 70 km offshore the south coastline of the island. Consequently, the temperature remained around 17 °C in the south coastline of the island. This large thermal difference between both faces is even larger at 0800 UTC (Fig. 7c), when the simulated temperature shows the higher values at the north face, around 31 °C (at the south face the temperature remained between 20 and 23 °C). From 1100 UTC the temperature began to decrease. As shown in Fig. 7d, during the afternoon the temperature shows normal values in both sides of the island.

Figs. 8a–d shows the temperature and water vapor–mixing ratio along the line AB showed in Fig. 8e. During the early morning on 23 March 2008, the warm and dry air mass is lifted over the relative cold and wet Mediterranean air mass, which remained at the south part of the island (Fig. 8a). At the south part of the island the temperature at sea level remained around 20 °C as a consequence of the influence of the cold sea air. However, at the north part the temperature increases, reaching 25 °C at many areas due to strong descending air not associated to a Foehn effect. The warming at the north coast of the island is associated to an air mass with the same characteristics of the African air mass that descends (vertical wind speed at the north side was around $-1\,\mathrm{ms}^{-1}$) once the colder Mediterranean air mass located at the south coast is overpassed. For this reason this air mass only affects the north part of the island.

Thermal difference between the north and the south coasts of the island increased in the coming hours. At 0700 UTC (Fig. 8b) the simulated temperature reaches 31 °C at Heraklion (north side) while at the south side the temperature remained around 20 °C. The largest value in the thermal difference between the north and the south sides of the island occurred around 1000 UTC (Fig. 8c). The simulated temperature at the north side reaches 31.8 °C at sea level, with $4.5\,\mathrm{g\,kg}^{-1}$ of water vapor–mixing ratio. At the south side, the air temperature reaches 21.3 °C and around $9\,\mathrm{g\,kg}^{-1}$ in the water vapor–mixing ratio. A change in the wind direction from 1400 UTC restored the normal values for both temperature and relative humidity. At 1600 UTC (Fig. 8d) the simulated temperature and water vapor–mixing ratio at both coasts are similar, around 22 °C and $9\,\mathrm{g\,kg}^{-1}$, respectively.

4 Potential risk and impacts of flash heats

Flash–heat events, a rapid increase of temperature, which lasts less than 2 consecutive days, could be associated with a variety of harm to human health, economic activities, and the environment.

According to data from the main Spanish electric company (Endesa), at midday on 27 of August 2010, a new record in electricity consumption was recorded; during few hours around 38000 MW were required in the whole country. The day before and after, consumption did not reach 23000 MW. The power network was working at 64 % over any other normal day for that period.

Moreover, most of the big wild fires in the Mediterranean are produced by a combination of high temperature and low relative humidity (Millan et al., 1998). Consequently, flash–heat events are likely to be one of the main risks in triggering wild fires because the drop in relative humidity and increase in temperature contribute to drying the vegetation.

Probably one of the most affected sectors during a flash–heat event is agriculture. Unlike what happens during a heat wave, when temperature and relative humidity changes slowly gradually and some measures (e. g. to irrigate to decrease water stress) can be taken in order to avoid its impact, during a flash heat the changes are more abruptly. For instance, during the flash-heat event on 27 August 2010 several regions in the northeast of the Iberian Peninsula lost around the 20 % of their grape production. Grapes are very sensitive to a sudden increase in temperature and drop in relative humidity, causing the fruit to lose a lot of internal water. After the event, the process cannot be restored and the production of wine is greatly disturbed in the quantity as well as the quality of wines (personal communication with the Torres wine company).

5 Conclusions

According to WMO and AMETSOC, as well as several national weather services, heat wave is defined as an abnormal period of higher temperatures over 2 or more days. In addition, AMETSOC defines a heat burst as a rapid increase in temperature that takes place over a period of minutes, usually associated to downstream flows occurring during storms or because of local Foehn effects. Thus, the events described in this paper are not a heat wave or burst. We propose to name this type of events flash heat.

The first analyzed flash heat occurred on 27 of August 2010 at the northeast area of the Iberian Peninsula due to a rapid and sudden advection of a warm and dry air mass

from the North Africa that affected this area for around 12 hours. The analysis of data from automatic weather stations located around Barcelona (northeast Iberian Peninsula) shows a rapid increase in temperature and a decrease in relative humidity after 0500 UTC. At 1300 UTC the temperature reached the maximum value, 39.3 °C, at the city center and 38.3 °C at the Fabra Observatory. The relative humidity decreased to 19 % at the city center and around 22 % at the Fabra Observatory. From 1500 UTC the temperature decreased; and at 1800 UTC it was less than 24 °C, i.e., within normal values for this season and time of the day.

WRF simulation shows a westerly flow over the Iberian Peninsula that advects warm and dry air over the Mediterranean coast, where the maximum temperature is simulated and in agreement with the observed values. This advection disappears at the northeast of the Iberian Peninsula and is replaced by an easterly flow that advects a relatively cold and wet air mass as it displaces the warm and dry mass onshore.

Applying the preliminary definition of flash heat to the historical temperature data series of Barcelona, we found that in the XIX century at least 13 episodes could be identified as flash heats.

The second analyzed event occurred on 23 March 2008 at the north face of the island of Crete. A rapid increase of temperature in Heraklion, a city located at the north coast of the island, caused by a strong downward flow, that keeps the characteristics of an air mass advected from Africa, has been studied and simulated. During almost 8 hours the temperature reaches higher than average values, and relative humidity show unexpected low values.. These recorded larger temperatures are due to the lift of a warm and dry African air mass caused by a colder Mediterranean air mass located at the south coast of Crete. This fact and the mountain waves that appeared due to the orography produce that the warm air mass only affected the north side of the island producing a large temperature difference between both coasts. From approximately 0000 to 1100 UTC on 23 March 2008 the temperature at Heraklion, and all over the north coast of the island reached more than 30 °C. From noon and early afternoon, when the southerly flow disappeared and ruled to easterly and southeasterly, the temperature decreased having usual values for this period of the year.

From the analyses shown in this paper, flash–heat events can be considered to define those warm events within Meso–β and Meso–γ scales lasting no more than 24 hours.

Acknowledgements. This project has been carried out by using the resources of the Supercomputing Center of Catalonia (CESCA) and it has been funded by the Spanish projects CGL2009–08609 and CGL2012–37416–C04–03. The NCEP images are from www.wetterzentrale.de. Observational data was provided by MeteoCat, AEMET and the Hellenic National Meteorological Service. We are also grateful to P. Nastos from the University of Athens for his helpful comments.

References

Egger, J. and Hoinka, K. P.: Fronts and orography, Meteor. Atmos. Phys., 48, 3–36, 1992.

Fotiadi, A., Hatzianastassiou, N., Drakakis, E., Matsoukas, C., Pavlakis, K. G., Hatzidimitriou, D., Gerasopoulos, E., Mihalopoulos, N., and Vardavas, I.: Aerosol physical and optical properties in the Eastern Mediterranean Basin, Crete, from Aerosol Robotic Network data, Atmos. Chem. Phys., 6, 5399–5413, 2006.

Frich, A., Alexander, L. V., Della-Marta, P., Gleason, N., Haylock, M., Klein Tank, A. M. G., and Peterson, T.: Observed coherent changes in climatic extremes during the second half of the twentieth century, Climate Res., 19, 193–212, 2012.

Glickman, T. S.: Glossary of Meteorology, American Meteorological Society, 2nd edn., 2000.

Hamilton, J. M., Maddison, D. J., and Tol, R. S. J.: Climate change and international tourism: a simulation study, Global Environ. Change, 15, 253–266, 2005.

Hassid, S., Santamourins, M., Linardi, A., Klitsikas, N., Georgakis, C., and Assimakopoulus, D. N.: The effect of the Athens heat island on air conditioning load, J. Energy Build., 32, 131–141, 2000.

Johnson, B. C.: The Heat Burst of 29 May 1976, Mon. Wea. Rev., 111, 1776–1792, 1976.

Jolly, W., Dobbertin, M., Zimmermann, N. E., and Reichstein, M.: Divergent vegetation growth responses to the 2003 heat wave in the Swiss Alps, Geophys. Res. Letters, 32, 18 409–18 418, 2005.

Karl, T. and Quayle, R. G.: The 1980 Summer Heat Wave and Drought in Historical Perspective, Mon. Wea. Rev., 109, 2055–2073, 1981.

Kaskaoutis, D. G., Kambezidis, H. D., Nastos, P. T., and Kosmopoulos, P. G.: Study on an intense dust storm over Greece, Atmos. Env., 42, 6884–6896, 2008.

Lise, W. and Tol, R. S. J.: Impact of climate on tourism demand, Clim. Change, 55, 429–449, 2002.

Maninns, P. C. and Sawford, B. L.: A model of katabatic wind, J. Atmos. Res., 36, 619–630, 1979.

Mazon, J., Barriendos, M., Prohom, M., Rodríguez, R., Blanch, A., and Ripoll, R.: Reconstruction of long temperature series of Barcelona, in: 11th EMS Annual Meeting, Berlin (Germany), 2011.

Meehl, G. A. and Tebald, C.: More intense, more frequent and longer lasting heat waves in the 21st centuri, Science, 13, 994–997, 2004.

Millan, M. M., Estrella, M. J., and Badenas, C.: Meteorological processes relevant to forest fire dynamics on the Spanish Mediterranean coast, J. Appl. Meteor., 37, 83–100, 1998.

Moulin, C., Lambert, C. E., and Dayan, U.: Satellite climatology of African dust transport in Mediterranean atmosphere, J. Geophys. Res., 103, 13 137–13 144, 1998.

Orlanski, I.: A rational subdivision of scales for atmospheric processes, Bull. Amer. Meteor. Soc., 56, 527–530, 1975.

Skamarock, W. C., Klemp, J. B., Dudhia, J., Gill, D. O., Barker, D. M., Duda, M., Huang, X.-Y., W., W., and Powers, J. G.: A Description of the Advanced Research WRF Version 3, Tech. Rep. TN–475+STR, NCAR, 2008.

Smoyer-Tomic, K. E., Khun, R., and Hudson, A.: Heat wave hazards: an overview of heat waves impacts in Canada, Nat. Hazards, 28, 465–486, 2003.

Steadman, R. G.: A universal scale of apparent temperature, J. Climate Appl. Meteor., 23, 1674–1687, 1984.

Trenberth, K. E., Jones, P. D., Ambenje, P., Bojariu, R., Easterling, D. Klein Tank, A., Parker, D., Rahimzadeh, F., Renwick, J. A., Rusticucci, M., Soden, B., and Zhai, P.: Observations: Surface and Atmospheric Climate Change, in: Contribution of Working Group I to the Fourth Assessment Report of the Intergovernmental Panel on Climate Change, 2007, edited by Solomon, S., Qin, D., Manning, M., Chen, Z. Marquis, M., Averyt, K. B., M., T., and Miller, H. L., Cambridge University Press, Cambridge, United Kingdom and New York, NY, USA, 2007.

Wakonigg, H.: The north foehn in the south–eastern Alpine border zone, Mitt. Oesterr. Geol. Ges., 132, 27–55, 1990.

Table 1. Three different scales of events linked to abnormal high temperatures. The scales are adapted from Orlanski (1975).

Event	Temporal scale	Spatial scale	Driving mechanism
Heat wave	From 2 to few weeks	Meso–α (200–2000 km)	General atmospheric circulation
Heat burst	Few minutes	Micro–β,γ (< 2 km)	Thunderstorms
Flash heat	1–24 h	Meso–β,γ (20–200 km)	General atmospheric circulation, Foehn effect

Table 2. Values of the average of the absolute maximum temperature, the average of the maximum monthly temperature and the 60$^{\text{th}}$ percentile of the average of the maximum monthly temperature recorded during the period 1961–1990 at the Barcelona–Fabra weather station (Barcelona)

Month	$\overline{T}_{max-abs}$ (°C)	$\overline{T}_{max}$ (°C)	$p60\overline{T}_{max}$ (°C)
July	32.6	27.6	28.6
August	31.6	26.7	27.6

Table 3. Most significant flash–heat episodes affecting Barcelona since 1780. Note that on the 27 of August 2010, the maximum temperature was 39.3 °C (24 °C in the early morning and 26 °C in the evening). T_{12-} and T_{12+} indicate the temperature 12 hours before and after the maximum temperature recorded (T_{max}), respectively.

Date	T_{max} (°C)	T_{12-} (°C)	T_{12+} (°C)	Wind direction
1/7/1790	36	23.5	25	SW
10/7/1820	34.4	21	26.5	SW
27/7/1843	35.5	23.5	24	SSW–SW
5/8/1846	35.5	26	27	S
15/7/1859	35	27	26	SSW–SW
17/8/1881	35.5	25	26	SSW
13/7/1896	36	21	22	SW

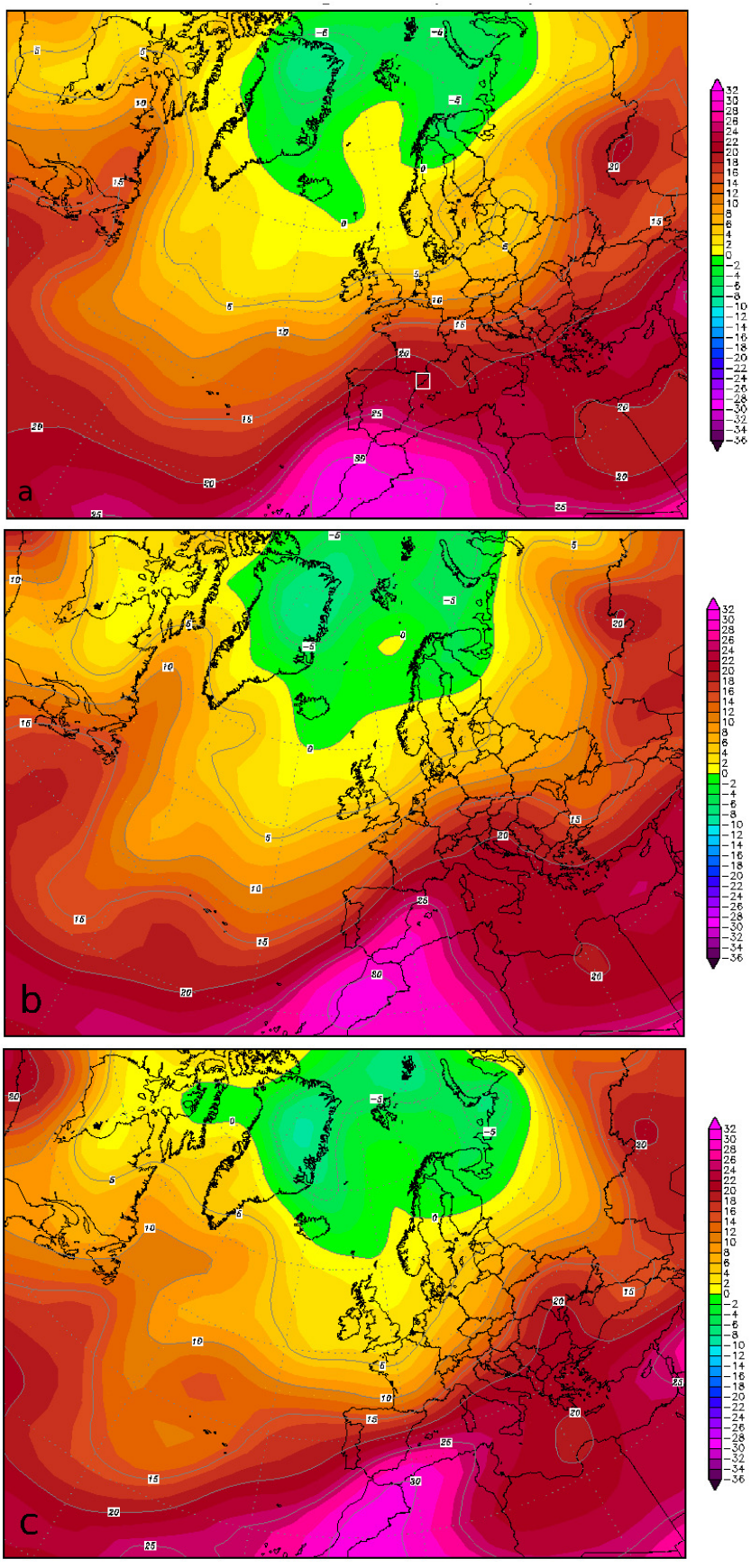

Fig. 1. Temperature at 850 hPa obtained by the NCEP reanalysis at 0000 UTC on (a) 26, (b) 27 and (c) 28 August 2010. The white square in (a) is centered over the first area under study.

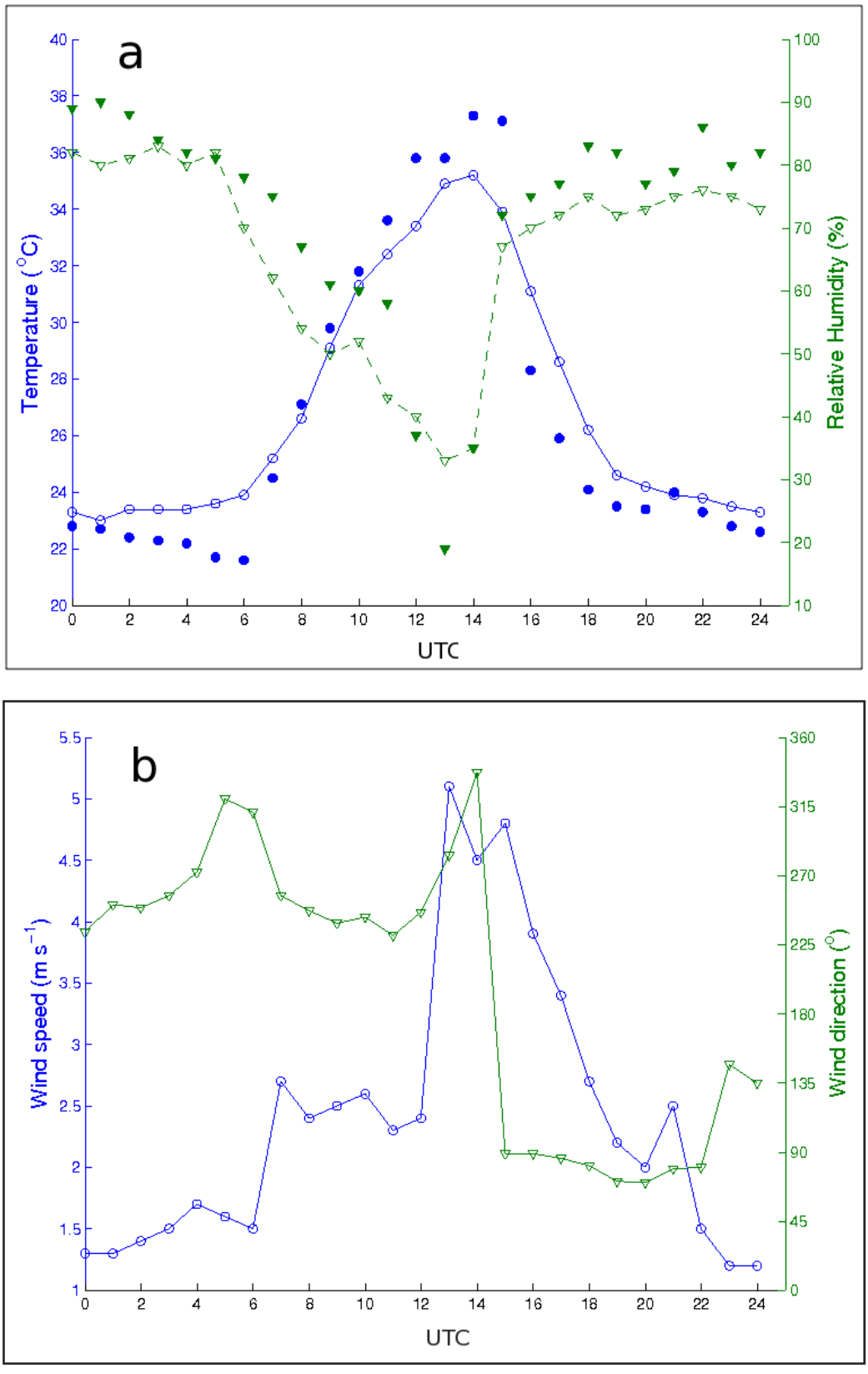

Fig. 2. Temporal evolution during 27 August 2010 of the 2–m (a) temperature (blue) and relative humidity (green) and (b) wind velocity (blue) and direction (green) observed at Barcelona–Fabra weather station (closed symbols) and simulated by the WRF model (line and open symbols).

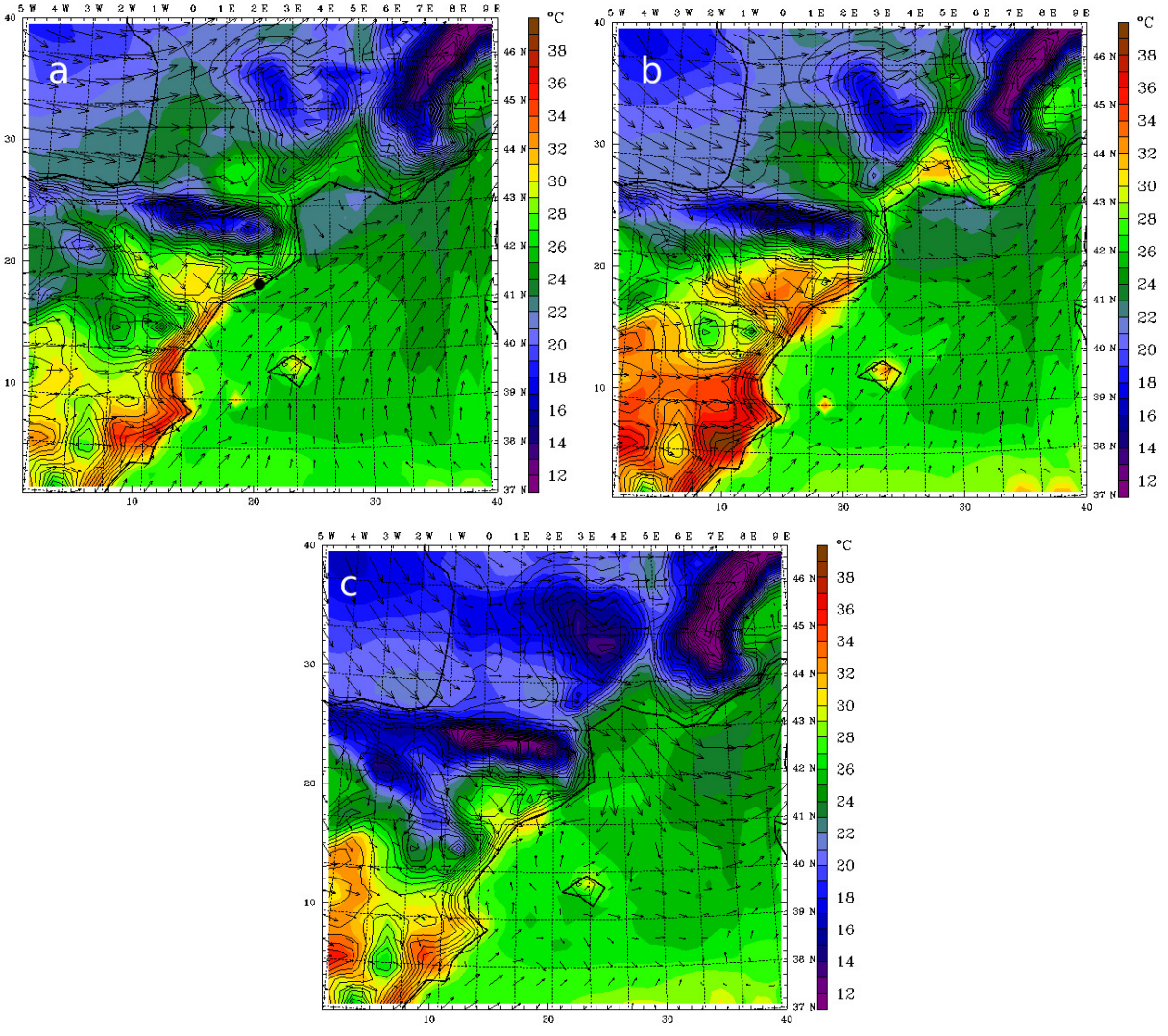

Fig. 3. Simulated 2–m temperature (color contour) and surface wind field (arrows) at domain 1 at (a) 1000, (b) 1500 and (c) 1800 UTC on 27 August 2010. The black point in (a) indicates the location of Barcelona.

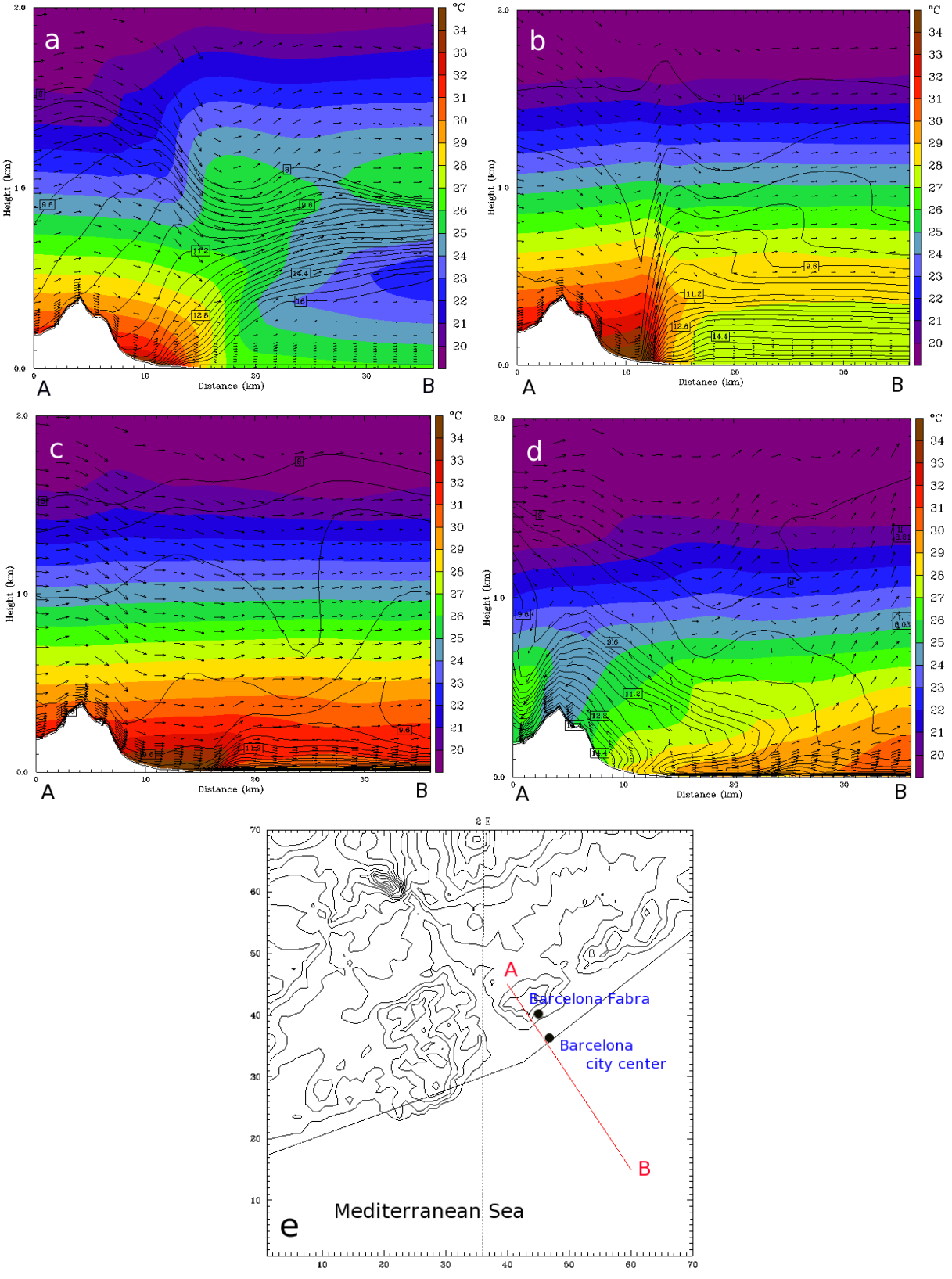

Fig. 4. (a–d) Vertical cross section along the line AB shown in (e) of the simulated temperature (color contour), water vapor–mixing ratio (black lines) and wind field (arrows) at (a) 1000, (b) 1200, (c) 1500, (d) 1800, and (e) 2000 UTC on 27 August 2010. (e) Orography of the smallest domain of the simulation.

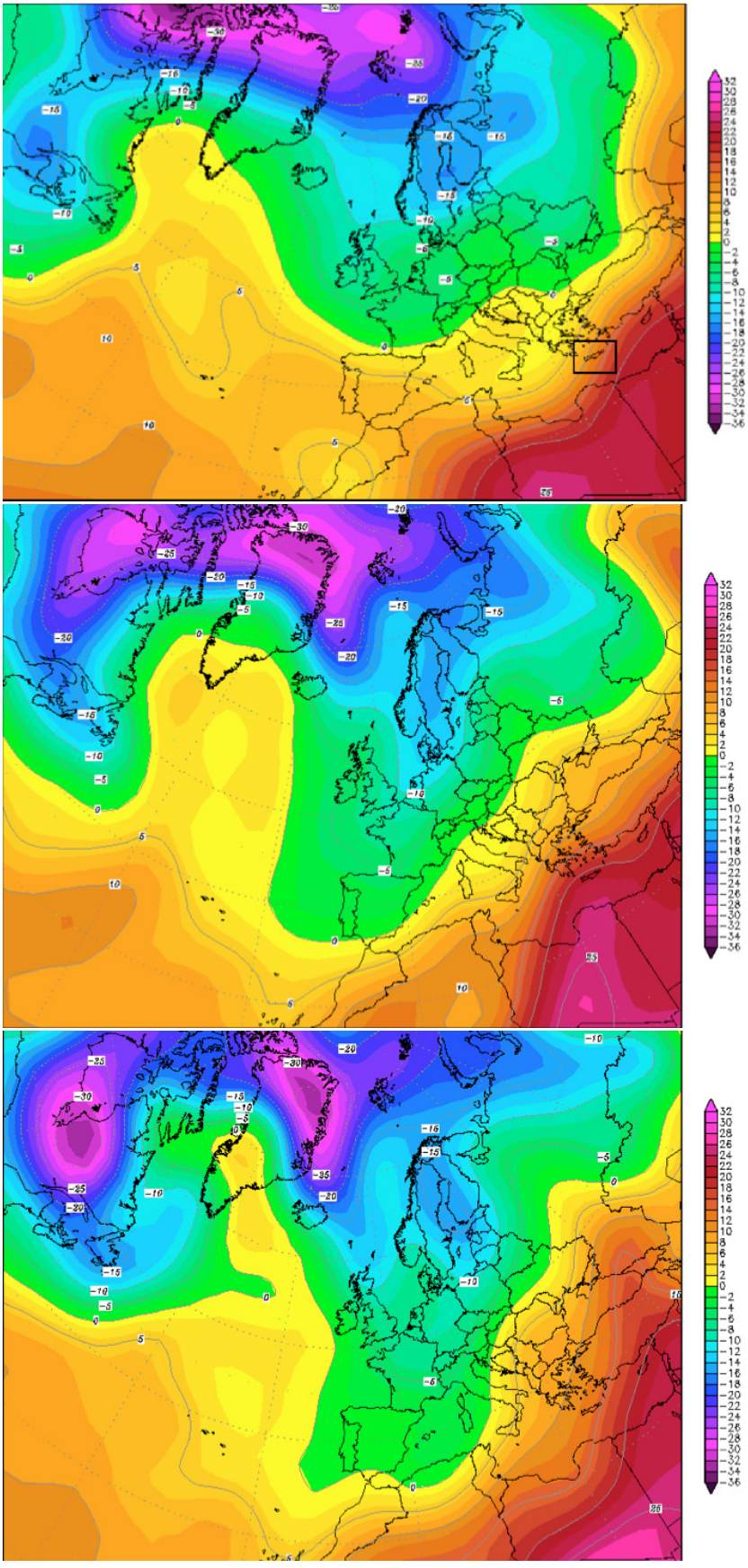

Fig. 5. Temperature at 850 hPa obtained by the NCEP reanalysis at 0000 UTC on (a) 22, (b) 23 and (c) 24 March 2008. The black square in (a) is centered over Crete.

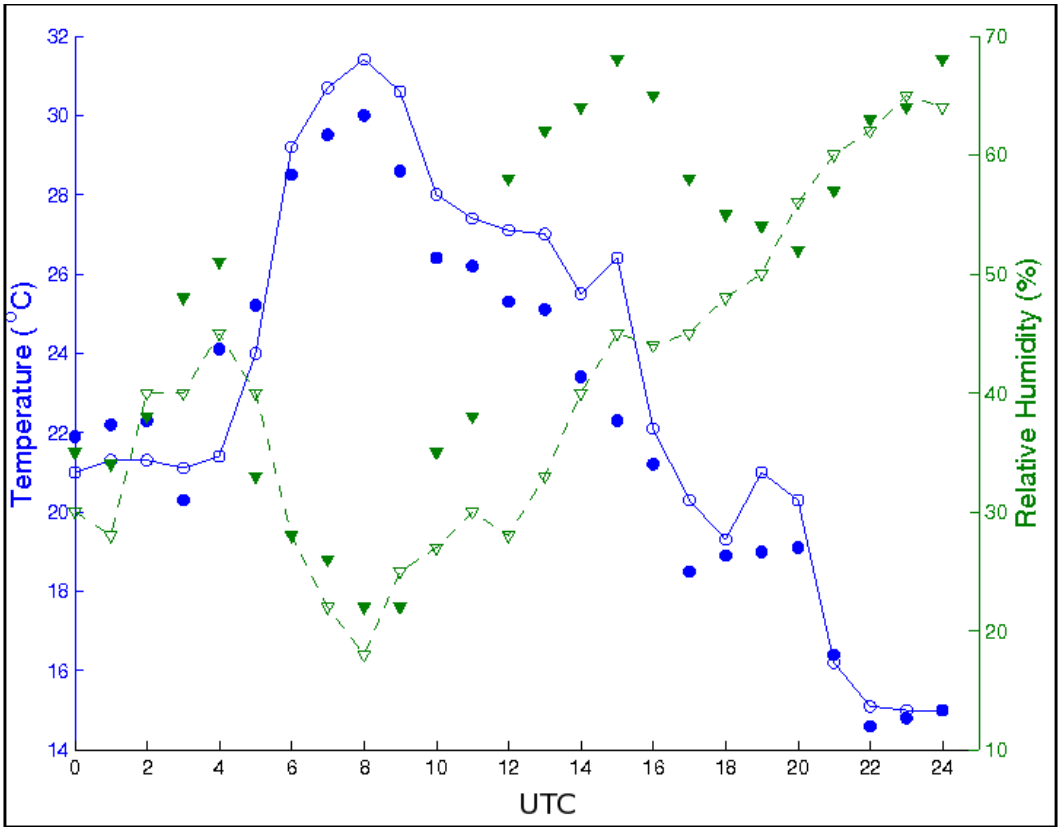

Fig. 6. Temporal evolution during 23 March 2008 of the 2–m temperature (blue) and relative humidity (green) observed at the Heraklion weather station (closed symbols) and simulated by the WRF model (line and open symbols).

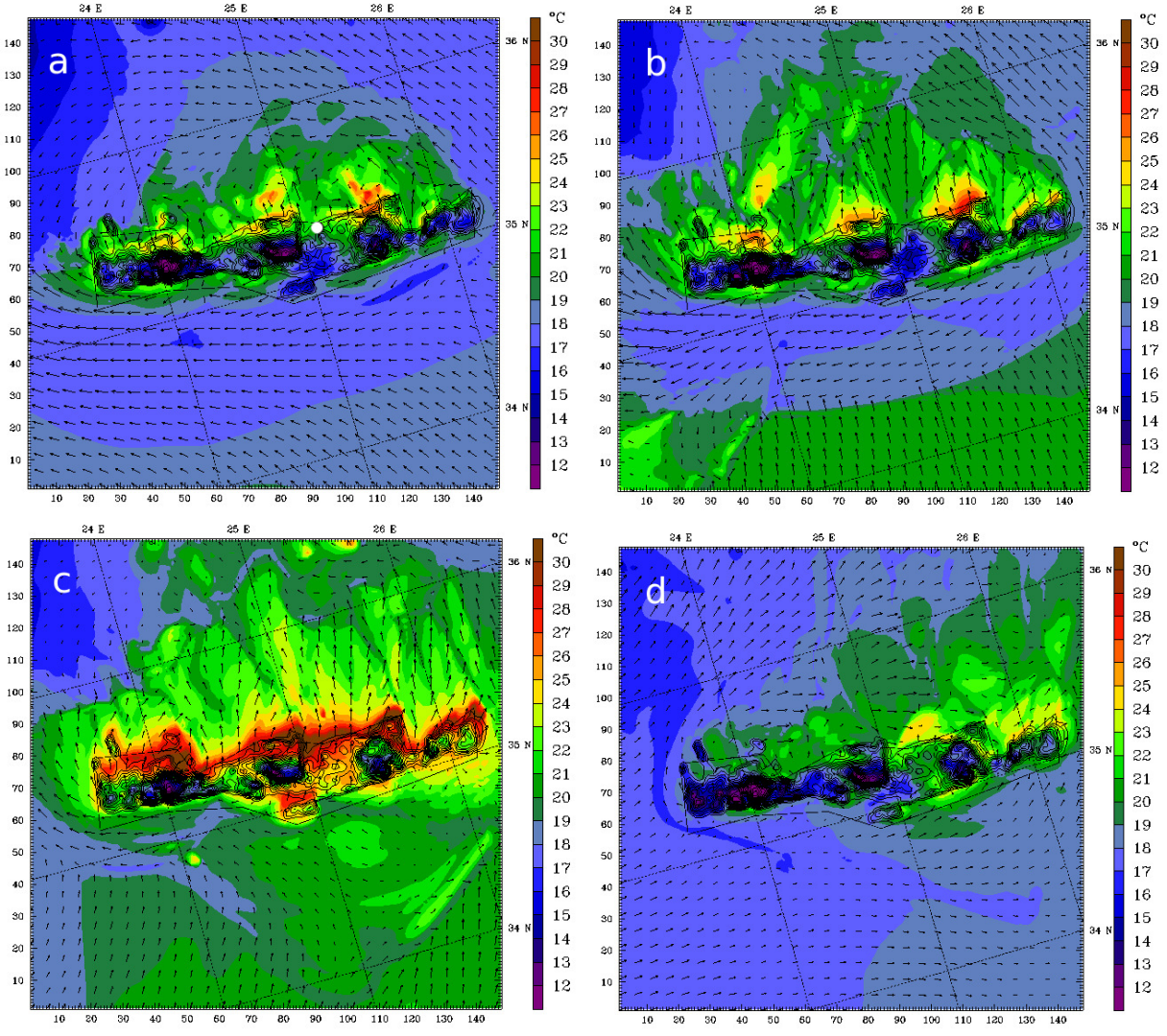

Fig. 7. Simulated 2–m temperature (color contour) and surface wind field (arrows) at domain 3 at (a) 0000, (b) 0400, (c) 0900 and (d) 1700 UTC on 23 March 2008. The white point in (a) indicates the location of Heraklion.

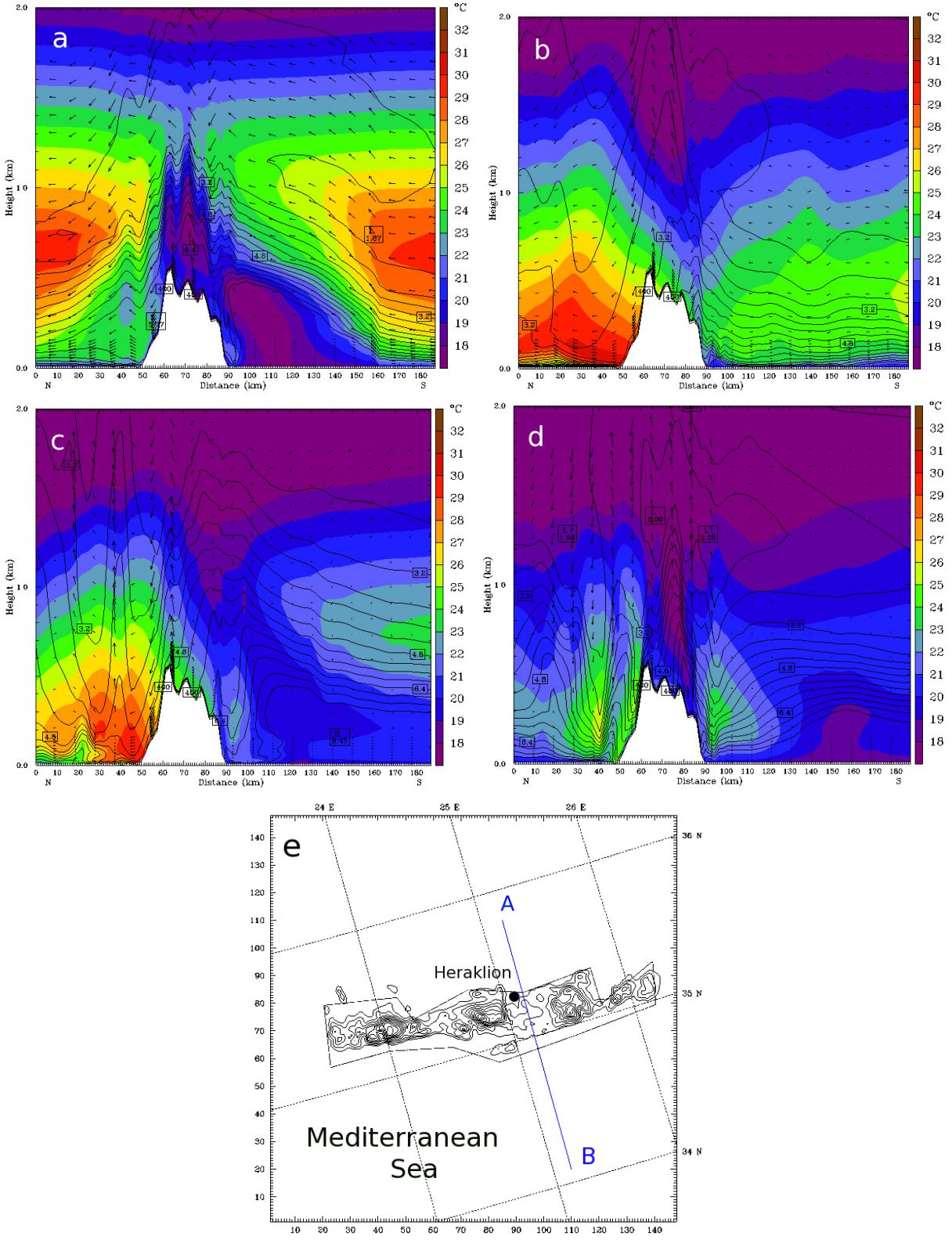

Fig. 8. (a–d) Vertical cross section along the line AB defined in (e) of the simulated temperature (color contour), water vapor–mixing ratio (line contour) and the wind field (arrows) on 23 March 2008 at (a) 0400, (b) 0700, (c) 1000 and (d) 1600 UTC. (e) Orography of the smallest domain of the simulation.